PHYSICAL REVIEW B VOLUME 30, NUMBER 12 15 DECEMBER 1984

Bremsstrahlung isochromat spectra and density-of-states calculations for the 3*d* and 4*d* transition metals

W. Speier, J. C. Fuggle,* R. Zeller, B. Ackermann, K. Szot,†
F. U. Hillebrecht, and M. Campagna‡
Institut für Festkörperforschung der Kernforschungsanlage Jülich, D-5170 Jülich, Federal Republic of Germany

(Received 23 July 1984)

We present the results of a systematic investigation of the empty electronic states up to 10 eV above E_F in the 3*d* and 4*d* transition metals with the use of bremsstrahlung isochromat spectroscopy (BIS). We compare these data to calculations of the unoccupied densities of states. The agreement between theoretical and experimental *d*-band widths and peak positions is quite good, although small discrepancies ($\lesssim 0.5$ eV) are found for the early transition metals. The unoccupied bandwidths are usually larger for the 4*d* than for the 3*d* metals and decrease from left to right across the Periodic Table, except where magnetic ordering of the 3*d* elements is important. A prominent step-like spectral feature observed at 7—10 eV above E_F in all spectra is attributed to a critical point in the band structure. The BIS spectra in the region up to 10 eV above E_F are not strongly affected by electron-energy-loss effects. Discrepancies between one-particle densities of states and the spectral response are smaller for BIS than for photoemission in these elements.

I. INTRODUCTION

One of the most significant developments in solid-state physics in the 1970s was the widespread use of photoelectron spectroscopy (PS) to study the occupied electronic states of condensed matter. However, the *unoccupied* electronic states in the range 0—10 eV above the Fermi level are known to have equal importance for understanding many physical properties of materials, such as optical or cohesive properties. This explains the development, similar to that in photoelectron spectroscopy in the last 15 years, which is now taking place in studies of the unoccupied states. Techniques such as bremsstrahlung isochromat spectroscopy (BIS),[1–21] inverse photoemission,[22–30] and even the old technique of x-ray-absorption spectroscopy (XAS) (see, e.g., Refs. 31—33) are being focused on the density of states (DOS) above the Fermi level (E_F). We present a systematic comparison of transition-metal BIS spectra and calculated DOS curves which gives a clear picture of the trends in the unoccupied states up to 10 eV above E_F. We focus on high-energy BIS because its analysis is comparatively straightforward, which is desirable for a general study.

The history of BIS can be traced back to the work of Duane and Hunt in 1915.[1] However, the first observation of structures in the short-wavelength limit of the bremsspectrum emitted when a monoenergetic beam of electrons bombarded a solid were probably those made in 1942 by Ohlin,[2] and interpreted as DOS features by Nijboer in 1946.[3] As shown in Fig 1, in the isochromat technique one varies the kinetic energy of the incident electrons, and by measuring the intensity of the light at one frequency one obtains information on the number and position of states above the Fermi level.[3] In the 35 years following Nijboer's work BIS was periodically rediscovered as a spectroscopic tool whose use was limited by vacuum capabilities in that era.[3–7,9–11] The regenesis of the technique dates to the start of ultrahigh-vacuum (UHV) measurements (see, e.g., Refs. 8 and 12—16) and the realization that an x-ray-photoemission—spectroscopy (XPS) monochromator could also be used for BIS studies.[16] However, much BIS work by Baer and others[16–19] has concentrated on lanthanides, actinides, and their compounds. BIS spectra of the pure transition metals have, surprisingly, not received proper attention in the last decade, in which workers have become aware of the importance of surface cleanliness. In view of the upsurge in interest in empty *d* states, especially for the understanding

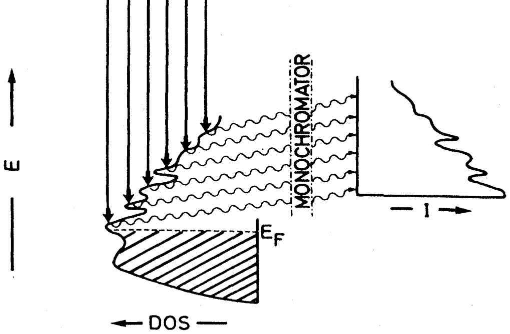

FIG. 1. Illustration of the principle of bremsstrahlung isochromat spectroscopy.

of alloy properties, we made rectification of this situation for the pure elements one of our aims.

There has also recently been an increase in studies of uv BIS,[22–30] now widely known as inverse photoemission.[27–30] The relationship between x-ray BIS and inverse photoemission is very similar to the relationship between x-ray and uv photoemission (XPS and UPS). XPS gives a picture which is rather closely related to the total density of states, and it is difficult to extract even rough information on the k dependence and dispersion of bands. The same is true for BIS. By contrast, in UPS and inverse photoemission angular dependence and momentum conservation can be used to build up a detailed picture of the k dependence of the bands. However, it is an arduous task to obtain the density of states using single crystals, and even for polycrystalline samples the k dependence of the radiative transition plays a role.[34] In addition, BIS is characterized by smaller electron-loss contributions at high energy than inverse photoemission, and by different matrix elements. We thus argue that the uv BIS and BIS at x-ray energies are complementary, not competitors.

A systematic study of transition-metal BIS spectra and calculated DOS curves is desirable to confirm the interpretation, in terms of the DOS, of the unoccupied energy bands. It is common practice to use eigenvalues obtained from ground-state theories to interpret experimental excitation spectra, but this procedure has no strict, formal justification.[35,36] The calculations are generally accepted to give a reasonable picture of ground-state properties (see, e.g., Refs. 35—40), but there are questions about the response of the crystal electrons when an electron is added or subtracted.[35,36] In photoemission of some metals, correlation effects lead to spectral weight in satellites and a shift of features in the "single-particle" region of the bands.[41] We know of no theoretical predictions for similar effects in BIS, except for strongly localized f orbitals,[19] and it is thus important that our systematic study of BIS spectra of transition metals include a search for such effects. We also know that the static exchange-correlation correction is reduced at high energies, so that band-structure calculations should really include an energy-dependence potential.[42,43] We have discussed this point elsewhere.[44] We will also discuss inelastic scattering of the primary beam. Because the primary beam in BIS has nearly the same kinetic energy as the electrons in the XPS valence band, the intensity of the energy-loss satellites in BIS and XPS should have *the same order of magnitude.*

The three major methods of studying unoccupied states are x-ray absorption (XAS), optical absorption in the visible and vacuum uv, and BIS. Each of these measurements implies a perturbation of the ground state of the system studied. This perturbation is smaller for BIS than for XAS because the Coulomb interaction between the extra valence electron above E_F and the valence electrons below E_F in BIS is smaller than the interaction between valence electrons and a *core* hole which is relevant to XAS. For instance, in Ni the effective hole-hole d-d interaction is ~ 2 eV,[45] while the $2p$-$3d$ interaction is ~ 6 eV.[46] In optical spectra, where joint densities of states are being measured, it has been known for a long time to be difficult to extract information on the unoccupied states of metallic samples.

To summarize our aims: we will attempt a systematic comparison of transition-metal BIS spectra with calculated DOS curves. With the help of this comparison, we will first try to separate out features relating to the physics of the BIS process and hence basically spurious in a solid-state study. We then assess how far the DOS calculations faithfully reproduce the observed spectral features of the empty states.

II. DOS CALCULATIONS

Our band-structure calculations of bcc and fcc metals were performed in the local-density approximation.[42,47] For bcc and fcc metals we used the Korringa-Kohn-Rostoker (KKR) method, with phase shifts up to $l=4$ and the first-principles self-consistent potentials of Moruzzi *et al.*[38,39] The densities of states are obtained by the tetrahedron method with 6144 tetrahedra in the irreducible part of the Brillouin zone. The high number of tetrahedra reduces the weight of possible spurious peaks due to band crossings. One point must be considered. This computed scheme is constructed to minimize the total energy with the Wigner-Seitz radius r_{WS} as a free variable. For Cu and Ag, r_{WS} is correctly reproduced to $\pm 1\%$, but for early transition metals r_{WS} can be 3% smaller than found experimentally. As the bandwidths and peak positions scale with r_{WS}^{-2}, a 3% decrease in r_{WS} corresponds to a 6% increase in calculated energy positions. For the tabulated bandwidths and peak positions given in this paper, we applied an energy rescaling to the theoretical values. We also performed calculations constructing self-consistent potentials for the experimental r_{WS} of V in order to satisfy ourselves that simple rescaling of the energy can be applied as a first approximation and is sufficient for our purposes.

The electronic structure of the hcp metals was calculated using the self-consistent augmented-spherical-wave (ASW) method.[48] This is linearized in energy and was optimized for the occupied bands so that results should be reasonable up to 10—15 eV above E_F. The DOS was obtained by a discrete sampling of 300 points in the Brillouin zone, which leads to a greater roughness in the hcp DOS's than for bcc and/or fcc metals, where 6144 tetrahedra were used. The hcp lattice constants were taken from experiment.[49]

For the ferromagnetic elements Fe, Co, and Ni, we made ferromagnetic calculations using standard methods.[39] For Cr, which is antiferromagnetic, we used a nonmagnetic calculation. The "up" and "down" bands in Cr are calculated to split ~ 1 eV in antiferromagnetic Cr,[50] which should broaden the Cr BIS spectrum noticeably with respect to our calculation, but should not be as serious as the magnetic effects in, for example, Fe. None of our calculations include relativistic effects, which is our main reason for limiting this study to $3d$ and $4d$ elements. Even for Ag, the heaviest element we studied, the relativistic corrections are known to amount to only a few tenths of an electron volt.[51]

In order to compare the theoretical density of states with the experimental spectra, it is essential to include broadening due to the experimental resolution (for these measurements, a Gaussian width of 0.7 eV) and the lifetime of the excited state. This lifetime broadening can be related to the imaginary part of the self-energy and is included by a convolution with an energy-dependent Lorentzian. van der Marel *et al.*[21] used a Lorentzian whose width increased linearly with energy above E_F $[0.09(E-E_F)]$ and a larger Gaussian width than we use here. We use a Lorentzian broadening of $0.25+0.09(E-E_F)$, with the 0.25-eV broadening at E_F probably being an instrumental contribution.

It is instructive to first consider some general features of the DOS for the three common crystal structures of the transition metals. We choose the DOS for the second-row metals Mo (bcc), Pd (fcc), Y (hcp), and Ru (hcp). The most prominent features of the DOS curves in Fig. 2 may be called the "*d* bands" because their wave functions have mainly *d* character. The states below and above the *d* band have mainly *s* (and *p*) character. The three major effects in DOS curves are the relative *s*-*d* positions, *d*-*d* overlap, and hybridization. In the early transition metals the centroid of the *d* bands is at a higher energy than that of the *s* bands, but in the later elements the *s* band moves up with respect to the *d* band and is eventually above the *d* band. The total *d*-band widths of the four elements illustrated in Fig. 2 are in the range 5—9 eV with Pd being much narrower than the others. It is a general trend for both first- and second-row transition metals that the bandwidths first increase by ~25% in going from Sc or Y to the middle of the series.[52,53] This happens because the approximately half-filled *d* shell is associated with high cohesion energy, a small atomic volume, and a large overlap of the *d* wave functions centered on neighboring sites. In the later transition metals the atomic volume varies less, but the *d* wave function shrinks due to the larger nuclear potential, and both the *d*-*d* overlap and the *d*-band width decrease. We return to the question of precise *d*-band widths below.

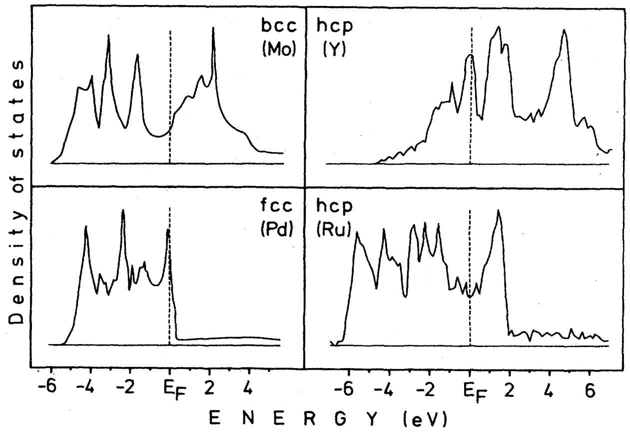

FIG. 2. Calculated DOS curves for Mo (bcc), Pd (fcc), Y (hcp), and Ru (hcp). The curves have been normalized to the maximum peak height.

Hybridization of the *s* and *d* bands is of general importance, and the so-called "*s*" and "*d*" bands are not pure. Hybridization is particularly important at the lower *d*-band edge in early transition metals. At the top of the *d* bands, hybridization effects are weaker but still present. They are stronger in hcp metals.[37]

When calculated state densities are compared, it is found that their overall appearance is similar for metals with the same crystal structures. For instance, in the case of the hcp structure we can recognize four main groups of peaks in Y and Ru the positions of which roughly scale with bandwidth. However, there are quite strong effects of hybridization in the bands, particularly for Y. This hybridization between *s* and *d* states lowers the energy at which we find the rapid rise in the state density associated with the *d* electrons, and weakens the lowest of the four hcp peak groups. The "characteristic" fcc and bcc DOS curves are similar but not precisely the same for all ele-

TABLE I. Position of major peaks in the unoccupied states (all values in eV). (Theor. denotes theoretical; Expt. denotes experimental.)

Element	Experimental BIS	Theoretical DOS	Average Theor. − expt.
Sc	1.8 3.8	1.4 3.5	−0.4
Ti	1.0 2.8	0.8 3.1	~0
V	2.3	2.5	+0.2
Cr	1.0	1.2	+0.2
Mn	1.4		
Fe	1.6	1.6	~0
Co	0.5	0.5	0.0
Ni	0.3	0.3	0.0
Y	2.0 5.4	1.3 4.6	−0.8
Zr	0.9 4.4	0.9 4.6	+0.1
Nb	3.5	3.4	−0.1
Mo	2.0	1.8	−0.2
Ru	1.2	1.3	+0.1
Rh	0.4	0.5	+0.1
Pd	0.2	0.1	−0.1

ments. We note here that the lower levels in the band have more bonding character, and the higher levels have more antibonding character. In the bcc metals such as Mo there is a broad minimum between these two groups of levels which arises from the bonding-antibonding interaction.[54] There is no such strong feature in the fcc or hcp metals.

Hybridization also complicates the interpretation of bandwidths. One criterion for estimation of bandwidths is inherent in the band-structure calculation, namely that at the bottom of the band, $d\psi/dr=0$ at the Wigner-Seitz radius r_{WS}, and at the top of the band the antibonding orbital density between the atoms at r_{WS} is zero, i.e., $\psi_{(r=r_{\mathrm{WS}})}=0$. However, this is not an ideal criterion for the spectroscopist because the strong mixing of s and d states at the band edges causes a steep rise in the partial density of d states outside these boundary conditions.[37,53] For this reason we use different criteria, and the widths, extracted by the method described in the Appendix and given in Table I, do not correspond precisely to those defined by the theoretical criteria above. Note, however, that these difficulties due to hybridization are greater at the bottom of the bands, in photoelectron spectra, because hybridization is greater there.

III. EXPERIMENTAL DETAILS

The measurements were performed on a modified XPS instrument, similar in principle to that of Lang and Baer,[16] but with 54 quartz crystals in the x-ray monochromator to increase its acceptance angle to 0.1 sr. The monochromator is set at 1486.7 eV, and the x-ray detector is a CsI photocathode and channeltron.[55] The total resolution, as measured by the width of the recorded step in the BIS spectra at E_F, is $\sim$700 meV. Standard multiscanning techniques were used. The high intensity and good signal-to-noise ratio in this instrument allows us to better judge the shape of the spectra after a short measurement (as short as 5 min) and to check for a buildup of contamination.

The samples were cleaned by scraping in a preparation chamber with a base pressure of 10^{-10} Torr. The pressure in the measurement chamber during measurements rose typically to 2×10^{-10} Torr as a result of electron-stimulated desorption by scattered electrons. The level of contamination was monitored by XPS and changes in the BIS spectra with time. Total contamination by all elements except hydrogen is estimated to be less than 0.25 monolayers. The time of measurement between successive cleaning cycles depended on the sensitivity to contamination. The most difficult samples were the early transition metals, where, after 40 min, distinct changes in the BIS spectra occurred. In these cases the cleaning was repeated every 10 min.

IV. RESULTS AND INTERPRETATION

We present the BIS spectra in Figs. 3 and 4 along with calculated total—density-of-states curves, broadened to account for instrumental and lifetime effects. The spectra from the late transition metals are generally in good agreement with those observed by other workers with similar photon energy.[7–10,13] This is not the case for the early transition metals measured until now,[5,6,11] which were often studied in a rather poor vacuum ($\sim10^{-7}$ Torr or worse) and at poorer resolution, and showed much less intensity at E_F than the present spectra. We cannot completely rule out the possibility of some contamination effects from the electron beam for the elements Sc or Y, but the spectra we present are certainly closer to the true "clean" spectra than anything we know of in the literature.

The general features that we observe in BIS are peaks near E_F, a broad structureless plateau at energies above the peaks, and a step about 7—10 eV above E_F. We can use the DOS to give assignments to the features. The peaks near E_F can be confidently ascribed to the empty transition-metal d band by comparison with the density of states, and the "step" is ascribed to a critical point.[56] This

TABLE II. Theoretical (theor.) values for occupied (W^-) and unoccupied (W^+) d-band widths, as compared to experimental (expt.) BIS values for W^+. All values in eV. The dual values given where the interpretation of experiment is ambiguous are a good guide to the accuracy.

Element	W^-(theor.)	W^+(theor.)	W^+(expt.)	W^+(theor$-$expt.)
Sc	1.7	4.0	4.4—4.7	-0.5
Ti	3.1	3.65	3.2—3.8	$\sim$0.0
V	3.2	4.0	3.4—3.8	$+0.4$
Cr	4.5	2.5	1.8—2.3	$+0.5$
Mn			$\sim$3.5	
Fe	5.3	2.6	2.9—3.5	-0.6
Co	5.5	1.15	1.4	-0.25
Ni	5.0	0.4	0.4	0.0
Y	2.0	5.3	6.1	-0.8
Zr	3.1	5.3	5.2—5.7	-0.1
Nb	3.5	5.6	5.2—5.9	0
Mo	5.4	3.9	3.9—4.5	-0.3
Ru	6.2	1.95	1.95	0.0
Rh	5.8	1.2	1.1	0.1
Pd	4.8	0.4	0.4	0.0

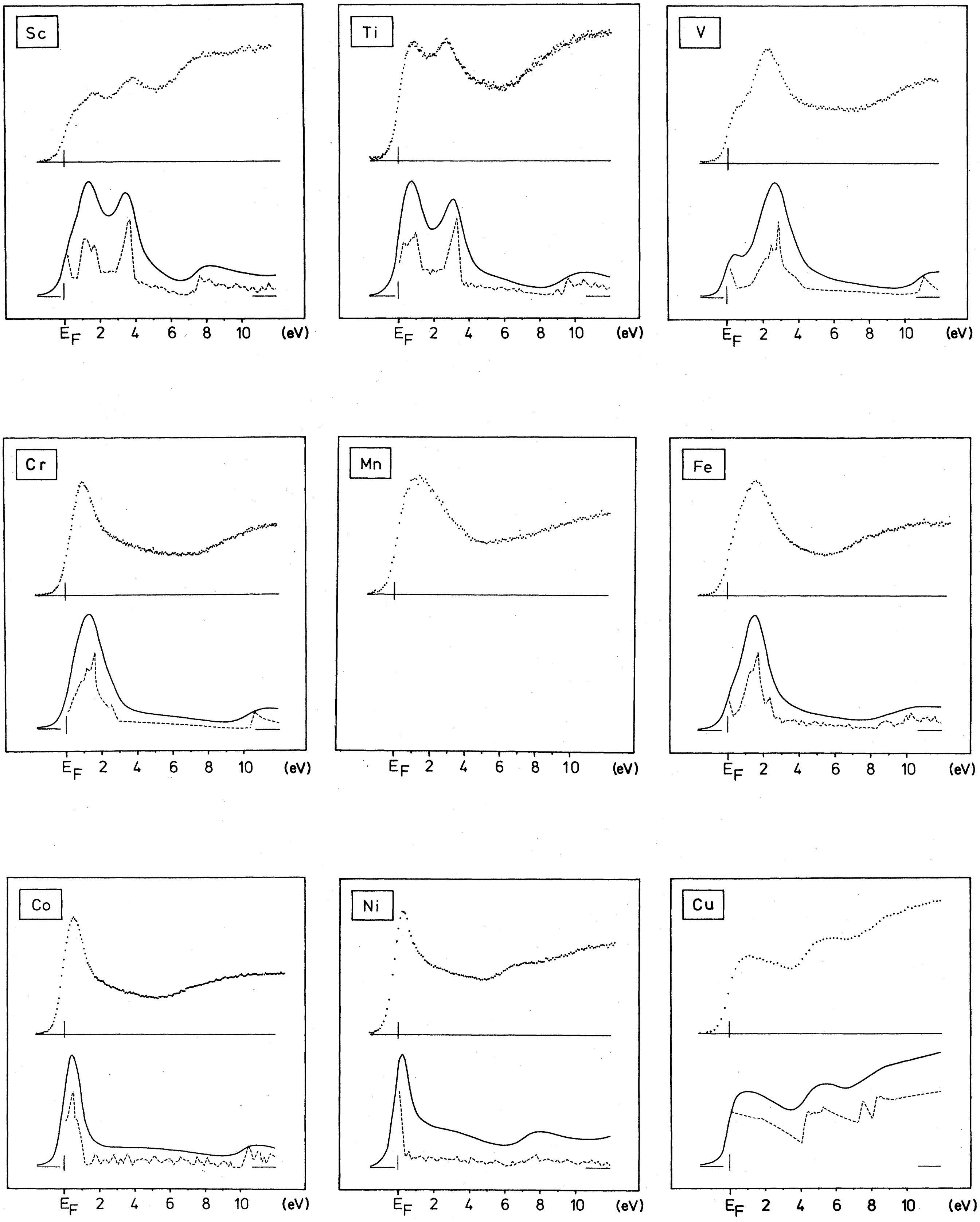

FIG. 3. BIS and DOS curves for the first-row transition metals and Cu. The dashed curves correspond to the unbroadened DOS, the solid lines to the DOS broadened with a Gaussian broadening of 0.7 eV and a Lorentzian broadening of $0.25+0.09(E-E_F)$ to simulate instrumental and lifetime broadening, respectively. The upper dotted curve in each case is the measured BIS spectrum.

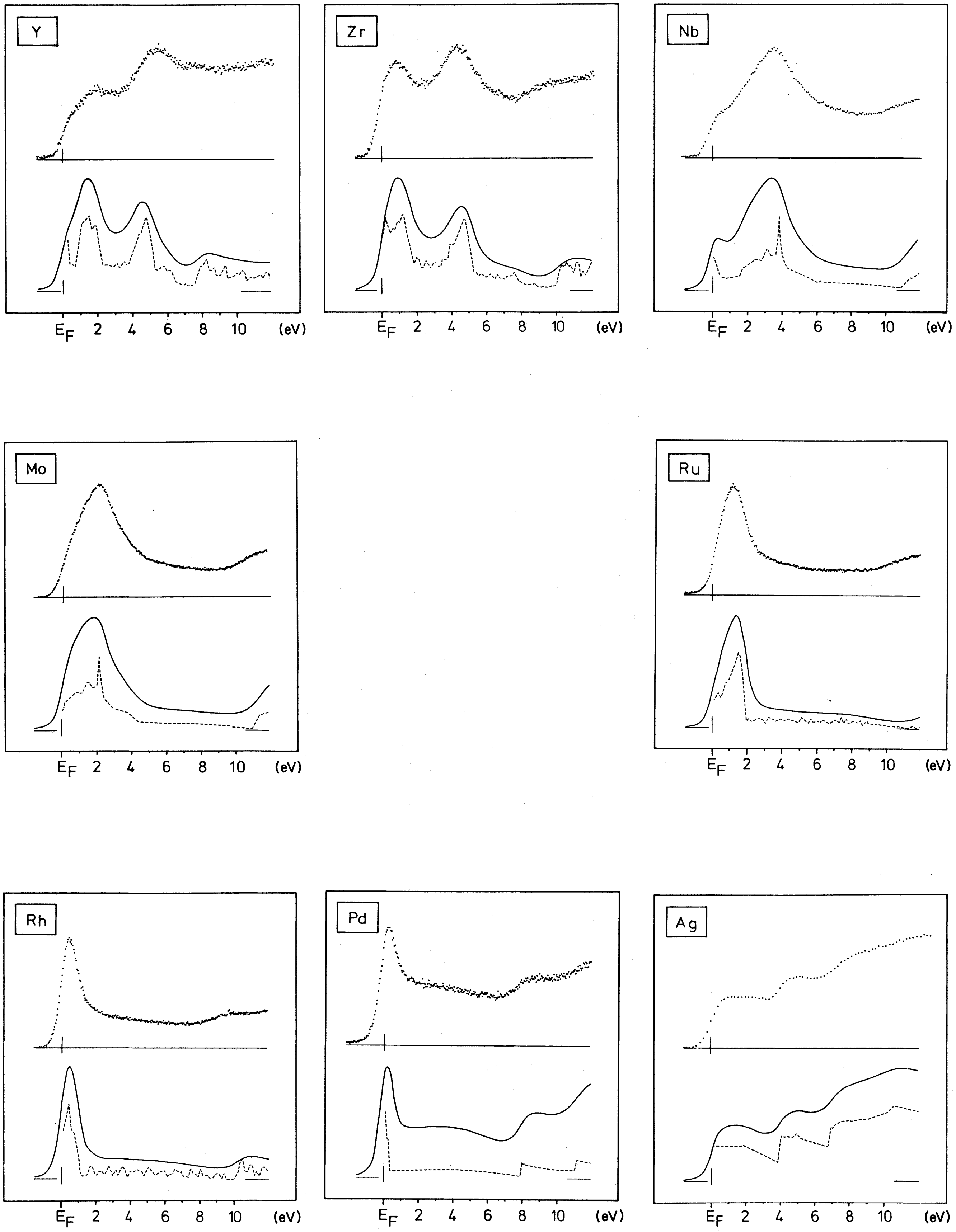

FIG. 4. BIS and DOS curves for the second-row transition metals and Ag. Symbols as for Fig. 3.

view is further supported by comparison with Cu and Ag, where no such prominent peaks are observed. We will start with a discussion of these *d* bands. Note that the other states above the *d* bands do have structure and that the bands probably contribute to the high-energy tail of the *d*-band region. For instance, when Cu and Ni are compared, it is seen that all the features are moved down by approximately 2 eV. The Cu *d* states are basically all occupied and, therefore, are below E_F. There is, however, even in Cu, a rise in the BIS intensity just above E_F, and this also occurs in Ni as an apparent tail on the Ni *d* band. This tail clearly complicates the estimation of *d*-band intensities in BIS discussed below, but is of secondary importance for the determination of peak positions and bandwidths.

The *d*-band peaks and widths found, by using the method described in the Appendix, in the unbroadened DOS curves and the experiments are shown in Tables I and II. There is generally good agreement between the BIS spectra and the broadened DOS curves, and this should not be forgotten as we try to isolate small discrepances and the reason for their existence. For instance, the number of major peaks found in the BIS spectra of Figs. 3 and 4 corresponds well to the number found in the broadened DOS above E_F. For Sc, Ti, V, and Zr two are found; for the other elements only one is found. We have even been able to detect, in BIS, the shoulders near E_F in the DOS curves in Sc, Y, V, and Nb which are due to peaks in the DOS which cross E_F. In addition, we find a distinct asymmetry of the Mo BIS peak which closely reflects that in the calculated DOS curve, and we find that for the bcc metals V, Cr, Nb, and Mo the Fermi level falls in a region of comparatively low DOS between the "bonding" and "antibonding" regions of the *d* band. We also find that the position of the *d*-band maximum in Fe is ~ 1.6 eV above E_F, in agreement with the ferromagnetic DOS curves and not in agreement with nonmagnetic calculations of DOS curves. As shown by Moruzzi *et al.*,[39] among others, paramagnetic calculations of the Fe DOS would give a peak much closer to E_F. Finally, we observe that the general trends in observed width of the unoccupied *d* states, W_+, is correctly given by the DOS curves.

When we look closely we find small discrepancies for the *d* bands in the early transition metals. It is not surprising that the small differences follow the same trend for *d* peak positions and estimated widths, as the higher-energy peak positions effectively determine the bandwidth measured. The calculated widths are ~ 0.5 and 0.8 eV too high for Sc and Y, respectively. In addition, we note that the "steps" due to critical points, at 7—10 eV above E_F are usually found at higher energies in the calculated DOS than in the observed BIS spectra (by $\sim$0—3 eV; see Table III). We tentatively attribute these effects to the dynamic exchange-correlation effects discussed elsewhere.[44]

In the region higher than ~ 5 eV above E_F, a partial-wave analysis of the calculated DOS shows a mixture of *s*, *p*, and *d* character at nearly all energies, with *p* being quite prominent. The BIS intensity in this region is higher with respect to the *d* band than in the DOS, and the steps are shifted. One must consider if this region is dominated by electron-energy-loss contributions arising from inelastic scattering of the primary beam. We discount this possibility because of the following reasons:

(1) The ratio of the intensity at 6—10 eV to the peak intensity is far higher than corresponding losses found in XPS;

(2) In general, neither XPS nor energy-loss— spectroscopy (ELS) measurements carried out in our laboratories show strong features at the correct energies to explain the step in the intensity 7—10 eV above E_F.

The experimental fact remains that the *d* bands of the early transition metals are weaker with respect to the plateau and step regions in BIS than in DOS calculations. The most likely explanation for this is that the cross section in the plateau and step regions is relatively high. We note, however, that this point should be checked by calculations of cross sections.

A calibration of intensities in BIS is difficult using the present apparatus because such intensities are very sensitive to the precise sample position and thickness. Attempts to normalize the absolute intensities with respect to one standard sample measured simultaneously were unsuccessful. The scattering in resulting intensities obtained when the same experiments were repeated with new samples was too large ($\sim 40\%$). The question of the intensity is, however, important, and thus for purposes of comparison we have adopted the approach of normalizing the spectra to the intensity minima above the *d* band, as shown in Fig. 5. The intensity in the minima is determined by the broad bands in this region, the DOS of which varies slowly with element. We then count the area of the *d* bands above a line drawn between the minimum and the Fermi level, as shown for Sc. This method gives a

TABLE III. "Critical-point positions" from theory (theor.) and the BIS experiment (expt.) (all values in eV, theory values corrected to expt. Γ_{WS}).

Element	Calculated position	Expt.	Theor. − expt.
Sc	7.4	6.6	0.8
Ti	9.3	8.1	1.2
V	10.1	9.7	0.4
Cr	9.8	9.1	0.7
Mn		~ 9	
Fe	8.3	6.8	1.5
Co	10.1	7.0	3.1
Ni	7	6.0	1
Cu	4.1	4.2[a]	0.1
Y	7.7		
Zr	10.0	8.9	1.1
Nb	10.7	10.4	0.3
Mo	10.7	10.2	0.5
Ru	12	~ 10.3	~ 1.7
Rh	10.1	8.7	1.4
Pd	7.9	7.8	0.3
Ag	3.8	3.8[a]	0
Avg.		3.77[b]	

[a] van der Marel *et al.* (Ref. 21).

[b] Reihl *et al.* (Ref. 30).

rough measure of the intensity derived from the *d* band, but has some inevitable drawbacks. Especially important is that subtraction of the straight-line background does not reliably remove the contribution of other bands, and the cross section of states at the "minimum" must vary with element. However, it is the most useful method we have for assessing broad trends in intensities.

We see in Fig. 5 that the relative *d*-band BIS intensity first rises to a maximum at about the middle of the transition-metal series, and then falls off again. Our curves of absolute intensities gave similar trends, but with more scatter. Even here the irregularities in the 3*d*-metal curve are probably a symptom of the inadequacies of the method used. Two effects are responsible for the general form of the curves. First, there is the rise in *d* cross section with increasing atomic number. This rise must be similar to the rise in cross section for XPS found both experimentally[57] and theoretically.[58] The second effect is the decrease in the number of *d*-band holes as one crosses the transition-metal series. This is the dominant effect in the late transition metals. Combining these two effects using Scofield's cross sections, and approximating the number of holes in the *d* band,[59] we obtain the theoretical curves shown in Fig. 5. These follow the form of the experimental curves quite well, but the differences along the 3*d* or 4*d* series are smaller than in experiment. This may be due to the separation of the *d*-band contribution from BIS or to the use of the minimum to normalize the curves. More work is obviously desirable on theoretical BIS cross sections. Scofield's photoemission cross sections are clearly a good approximation for *d*-band BIS, but they do rely on atomic wave functions, not solid-state wave functions, and they do not take into account the variation of wave function and, hence, cross sections with position in the band. We also need a guide to the cross sections for the *s*-*p* contribution of the BIS, both in the band and above it. Only when these results are available will we be able to give a fully reliable separation of *d*-band BIS intensities.

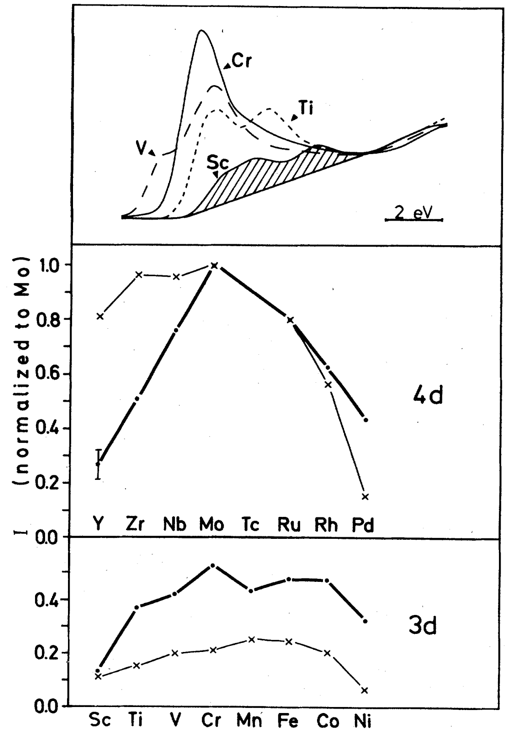

FIG. 5. Top: The BIS spectra of Sc—Cr normalized to the intensity minimum above the *d* band. Bottom: Variation of BIS *d*-band intensities (dots) and calculated intensities (crosses) for transition metals. The experimental values on the *y* axis are the *d*-band area divided by the intensity at the minimum, ~6 eV above E_F, and normalized to Mo=1. The 3*d* curve would be reduced by ±20% if we were to use absolute intensities.

In analogy to matrix-element effects in XPS from alloys, we wish to illustrate the importance of the cross section effects for BIS of alloys and compounds. As a random example, we choose ScPd, where we might expect the Sc contribution to the empty *d* band to dominate BIS because Sc has 8.5 holes as compared to 0.4 in Pd. Nevertheless, the lesson we learn from Fig. 5 is that the disparity in cross sections per hole is so great that the 0.4 Pd holes should actually be the determining factor in the shape of the BIS of such an alloy (also see Ref. 59).

V. CONCLUDING REMARKS

Our most general conclusion is that the agreement between calculated one-particle DOS curves and BIS of the transition-metal *d* bands is better than that between one-particle DOS and photomission curves. Thus, for instance, Eastman *et al.*[60] find discrepancies in the *occupied* *d*-band widths of 0.4, 0.9, and ~1.5 eV for Fe, Co, and Ni, respectively, in photoemission. The Ni discrepancy, in particular, is larger than anything we find. In addition, we note that the XPS spectra of early transition metals also gives curves which are very distorted with respect to the one-particle DOS curves.[61] In these metals it is very difficult to even recognize the bottom of the bands because of the long tail arising from many-body electron-hole—pair creation of the Doniach-Šunjić type.[61,62] Furthermore, there are no obvious satellites due to localized d^{n+1} states analogous to the f^2 peaks in Ce BIS (see, e.g., Ref. 19), and nor are there any satellites analogous to the d^8 structure in XPS of Ni valence bands.[41] The only possible candidate for strong many-body effects which we see in the spectra is the very high BIS intensity in the region immediately above the *d* bands, but it is necessary to make a thorough study of the single-particle matrix elements before one should speculate about many-body effects in the spectral response here.

For the *d*-band region, clearly *a one-particle DOS calculation* is a good starting point for rationalization of the spectra. We note that this behavior is quite different from that of the rare earths or actinides,[17–19] or even for the Mn 3*d* levels of Mn impurities in a Ag matrix,[63] where strong atomic multiplet effects dominate the spectral features.

Only one of the BIS spectra stands out for its exceptional width and broad, featureless peak just above or at E_F, namely Mn. Mn has an unusual crystal structure (α-Mn) with 58 atoms per unit cell, which is not very amenable to band-structure calculations. However, we note that in the absence of such calculations it is difficult at present to assess the relative importance of single-particle and atomic (multiplet) effects. The latter are expected to be large because of the high stability of the d^5 configuration.

ACKNOWLEDGMENTS

We thank J. Keppels for technical assistance and J. Kübler for access to the programs to calculate the DOS for hcp elements. We also thank P. Dederichs and J. Müller for fruitful discussions. One of us (K. S.) gratefully acknowledges financial support from the Deutscher Akademischer Austauchdienst, and hospitality and support from the Institut für Festkörperforschung der Kernforschungsanlage (KFA) Jülich.

APPENDIX

Estimation of precise bandwidths from experimental spectra with instrumental and lifetime broadening is nontrivial, partially subjective, and there is no "correct" way to do it. We will give details of the method we used to obtain numbers suitable for discussion, and if other people should need another measure more suitable to their uses, the spectra are also presented. We started by arguing that the long tail of very low partial-d-wave character has little significance, and so we seek the limits within which most of the transition-metal d character is found. This point is usually easily found in the unbroadened theoretical curve; for instance, in V we would set it at ±4.0 eV, as indicated by an arrow in Fig. 6. If we then look at the height of the broadened curve at 4.0 eV, we find it to be at 25% of the high-energy flank in V. In other elements it may be higher. We then seek the corresponding point in the experimental spectrum and define this as the experimental width. For instance, as shown in Fig. 6 we estimate the experimental width of the unoccupied d band to be 3.4—3.8 eV, which is slightly lower than the theoretical value. This method seems to be sensible and reliable for all the elements studied and makes use of the fact that we do have computed band shapes for all elements except Mn. This use of the calculated DOS seems fair because no one would argue about the ability of the computing scheme to reproduce the band shape. The uncertainties arise because of scaling factors, energy-dependent potential arguments, and the application of a one-particle DOS to spectroscopy, all of which affect the exact positions of the features much more than the overall shape.

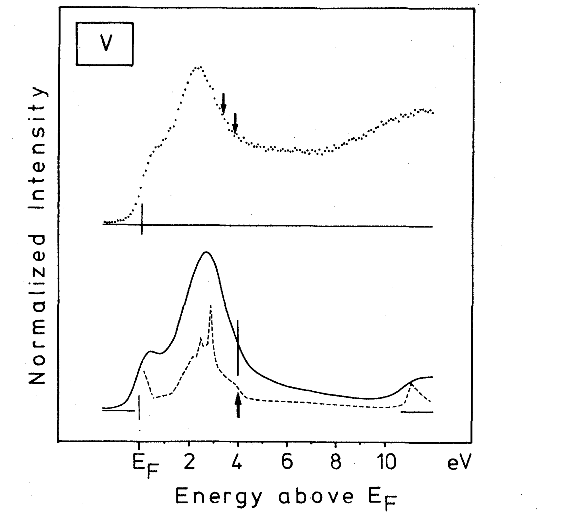

FIG. 6. Illustration of the method used to estimate experimental bandwidths. For further details, see text.

---

[*] Present address: Laboratorium voor Fysische Chemie, Faculteit der Wiskunde en Natuurwetenschappen, Universiteit van Nijmegen, Toernooiveld, 6525 ED Nijmegen, Nederland.

[†] Permanent address: Institute of Physics, Silesian University, Katowice, Poland.

[‡] Physikalisches Institut der Universität zu Köln, D-5000 Köln 41, Federal Republic of Germany.

[1] W. Duane and F. L. Hunt, Phys. Rev. **6**, 166 (1915).

[2] P. Ohlin, Ark. Mat., Astron. Fys. A **29**, 3 (1942).

[3] B. R. A. Nijboer, Physica (Utrecht) **12**, 461 (1946).

[4] K. Ulmer, Phys. Rev. Lett. **3**, 514 (1959); P. Johansson, Ark. Fys. **18**, 329 (1960).

[5] S. Bergwall and R. T. Tyagi, Ark. Fys. **29**, 439 (1965).

[6] H. Merz and K. Ulmer, Z. Phys. **210**, 92 (1968); **212**, 435 (1968); G. Böhm and K. Ulmer, *ibid.* **228**, 473 (1969).

[7] J. Eggs and K. Ulmer, Z. Phys. **213**, 293 (1968).

[8] R. Turtle and R. Liefeld, Phys. Rev. B **7**, 3411 (1973).

[9] H. Merz, in *Band Structure Spectra of Metals and Metals and Alloys*, edited by D. J. Fabian and L. M. Watson (Academic, London, 1973), p. 543.

[10] R. Kleber, Z. Phys. **264**, 309 (1973).

[11] H. Föll, Z. Phys. B **26**, 329 (1977).

[12] P. E. Best and C. C. Chu, Jpn. J. Appl. Phys. **17**, 317 (1978).

[13] F. Riehle, Phys. Status Solidi B **98**, 245 (1980).

[14] C. C. Chu and P. E. Best, Phys. Rev. B **12**, 4575 (1975); **19**, 3414 (1979).

[15] V. Dose and H. Scheidt, Phys. Status Solidi **103**, 247 (1981).

[16] J. K. Lang and Y. Baer, Rev. Sci. Instrum. **50**, 221 (1979).

[17] Y. Baer and J. Schönes, Solid State Commun. **33**, 885 (1980).

[18] J. K. Lang, Y. Baer, and P. A. Cox, J. Phys. F **11**, 121 (1981).

[19] F. U. Hillebrecht, J. C. Fuggle, G. A. Sawatzky, M. Campagna, O. Gunnarsson, and K. Schönhammer, Phys. Rev. B **30**, 1777 (1984).

[20] F. U. Hillebrecht, J. C. Fuggle, G. A. Sawatzky, and R. Zeller, Phys. Rev. Lett. **51**, 1187 (1983).

[21] D. van der Marel, G. A. Sawatzky, R. Zeller, F. U. Hillebrecht, and J. C. Fuggle, Solid State Commun. **50**, 47 (1984).

[22] V. Dose, Appl. Phys. **14**, 117 (1977).

[23] P. O. Nilsson and C. G. Larsson, Jpn. J. Appl. Phys. **17**, 144 (1978).

[24] G. Denninger, V. Dose, and H. Scheidt, Appl. Phys. **18**, 375 (1979).

[25] V. Dose and G. Reusing, Appl. Phys. **23**, 131 (1980).

[26] V. Dose, Th. Fauster, and H. Scheidt, J. Phys. F **11**, 1801

(1981); F. Himpsel and Th. Fauster, Phys. Rev. Lett. **49**, 1583 (1982).

[27] J. Pendry, Phys. Rev. Lett. **45**, 1356 (1980).

[28] G. Chauvet and R. Baptist, J. Electron. Spectrosc. Relat. Phenom. **24**, 255 (1981).

[29] D. P. Woodruff, N. V. Smith, P. D. Johnson, and W. A. Royer, Phys. Rev. B **26**, 2943 (1982).

[30] B. Reihl and R. R. Schlitter, Phys. Rev. B **29**, 2267 (1984).

[31] I. V. Azaroff and D. M. Pease, in *X-Ray Spectroscopy,* edited by L. V. Azaroff (McGraw-Hill, New York, 1974), p. 284.

[32] J. E. Müller and J. W. Wilkins, Phys. Rev. B **29**, 4331 (1984).

[33] R. D. Leapman, L. D. Grunes, and P. L. Fejes, Phys. Rev. B **26**, 614 (1982), and references therein on experimental work.

[34] V. Dose and Th. Fauster, Solid State Commun. **50**, 67 (1984).

[35] O. Gunnarsson and R. O. Jones, Phys. Scr. **21**, 394 (1980), and references therein.

[36] A. R. Williams and V. von Barth, in *Theory of the Inhomogeneous Electron Gas,* edited by S. Lundqvist and N. H. March (Plenum, New York, 1983), p. 189, and references therein.

[37] O. Jepsen, O. Krogh-Anderson, and A. R. Mackintosh, Phys. Rev. B **12**, 3084 (1975), and references therein.

[38] V. L. Moruzzi, A. R. Williams, and J. F. Janak, Phys. Rev. B **15**, 2854 (1977).

[39] V. L. Moruzzi, J. F. Janak, and A. R. Williams, *Calculated Electronic Properties of Metals* (Pergamon, New York, 1978), and references therein.

[40] A. R. Mackintosh and O. K. Anderson, in *Electrons at the Fermi Surface,* edited by M. Springford (Cambridge University Press, Cambridge, 1980), p. 149.

[41] J. C. Fuggle, F. U. Hillebrecht, R. Zeller, Z. Zołnierek, P. A. Bennett, and Ch. Freiburg, Phys. Rev. B **27**, 2145 (1982). For literature on photomission satellites, see Refs. 1–18 in this paper.

[42] B. I. Lundqvist, Phys. Status Solidi **32**, 273 (1969); L. Hedin and B. I. Lundqvist, J. Phys. C **4**, 2064 (1971).

[43] P. O. Nilsson and C. G. Larsson, Phys. Rev. B **27**, 6143 (1983).

[44] W. Speier, R. Zeller, and J. C. Fuggle (unpublished).

[45] P. A. Bennett, J. C. Fuggle, F. U. Hillebrecht, A. Lenselink, and G. A. Sawatzky, Phys. Rev. B **27**, 2194 (1983).

[46] F. U. Hillebrecht, J. C. Fuggle, P. A. Bennett, Z. Zołnierek, and Ch. Freiburg, Phys. Rev. B **27**, 2179 (1983).

[47] W. Kohn and L. S. Sham, Phys. Rev. **140**, A1133 (1965).

[48] A. R. Williams, J. Kübler, and C. D. Gelatt, Jr., Phys. Rev. B **19**, 6094 (1979).

[49] C. Kittel, in *Introduction to Solid State Physics,* 5th ed. (Wiley, New York, 1976), p. 31.

[50] J. Kübler, J. Magn. Magn. Mater. **20**, 277 (1980).

[51] N. E. Christensen, J. Phys. F **8**, L51 (1978).

[52] V. Heine, Phys. Rev. **153**, 673 (1967).

[53] D. G. Pettifor, J. Phys. F **7**, 613 (1977), and references therein.

[54] J. Friedel in *Physics of Metals I. Electrons,* edited by J. M. Ziman, (Cambridge University Press, Cambridge, 1969), p. 340.

[55] F. U. Hillebrecht, Ph.D. thesis, Köln Universität, 1983; Bericht der Kernforschungsanlage Jülich No. 1928, 1984 (unpublished).

[56] The concept of an analytical critical point, where the group velocity of the electrons is zero, was first explored by L. van Hove for lattice vibrations [Phys. Rev. **89**, 1189 (1953); also see J. C. Philips, Phys. Rev. **104**, 1263 (1956) or most books on solid-state physics]. Topological considerations lead to the conclusion that there are four types of van Hove singularities at maxima (one), saddle points (two), and minima in $\vec{k}$ space. We normally refer to critical points at minima in the energy bands here. A fuller discussion of the behavior of the bands around the critical points would be more appropriate to a study by lower-energy *k*-resolved inverse photoemission spectroscopy (KRIPES).

[57] J. C. Fuggle, D. J. Fabian, and S. Affrossman, in *X-Ray Spectra and Electronic Structure of Matter,* edited by A. Faessler and G. Wiech (Fotodruck Frank OHG, Munich, 1973), Vol. II, p. 164.

[58] J. H. Scofield, J. Electron. Spectrosc. Relat. Phenom. **8**, 129 (1976).

[59] If we wish to judge the contribution of the *d* bands to the spectra, then the best procedure is to assume that the *d* bands hold 10 electrons and then count the number of electrons or holes. Here, for instance, we just used the number of 8.5 *d*-band holes for Sc or Y and 0.6 holes for Ni (0.4 for Pd) and extrapolated for elements in between. Inaccuracies in this procedure are negligible for Fig. 5. Of course, the procedure is different if we wish to analyze the contribution of the *d* wave to the BIS spectrum; then we must take hybridization into account. For instance, it is well known that although Ni has 9.4 electrons in the 3*d* band, the 3*d*-electron count is only approximately 8.8, and the *sp* waves contribute ~0.6 electrons to the 3*d*-band population. If we wish to analyze the 3*d* contribution to the *d*-band region up to ~0.4 above E_F, then the 0.6 holes in the *d* band are relevant. If we wish to analyze the *total* 3*d* contribution to BIS, then the relevant number is $10-8.8=1.2$ holes. These distinctions are especially important in analysis of spectra of alloys.

[60] D. E. Eastman, J. F. Janak, A. R. Williams, R. V. Coleman, and G. Wendin, J. Appl. Phys. **50**, 7423 (1979).

[61] H. Höchst, P. Steiner, G. Reiter, and S. Hüfner, Z. Phys. B **42**, 199 (1981).

[62] S. Doniach and M. Šunjić, J. Phys. C **3**, 285 (1970).

[63] D. van der Marel, G. Sawatzky, and F. U. Hillebrecht, Phys. Rev. Lett. **53**, 206 (1984).